# Development of Low-NOx DME Multi-Port Burner*

Ryosuke MATSUMOTO**, Mamoru OZAWA**, Isao ISHIHARA**,
Shingo SASAKI** and Masahiro TAKAICHI**

This study focuses on the fundamental characteristics of DME (Dimethyl Ether) combustion, aiming at the development of low-NOx multi-port burner suitable for the tube-nested combustor. In the tube-nested combustion, the water tubes are moved into the furnace closely to the burner to cool the burning flame directly in the field of burning reaction leading to NOx reduction. To prevent the unburned combustibles emission, the diffusion burner used in the tube-nested combustor needs a high performance of the fuel-air mixing. Multi-port burner consists of a fuel-port and surrounding multi-air-ports, which induce a strong re-circulation flow. Thus the fuel-air mixing is enhanced so that the thermal NOx and CO emissions are significantly reduced. The NOx emission of the DME from the co-axial diffusion burner was over 130 ppm at 0% $O_2$. On the other hand, NOx emission of DME from the multi-port burner was reduced to 60 ppm at 0% $O_2$. With the help of the tube-nested combustion, NOx emission of DME was further reduced to 20 ppm at 0% $O_2$.

***Key Words*:** DME, Diffusion Combustion, Tube-Nested Combustor, NOx Reduction, Boiler

## 1. Introduction

Increasing attention has been focused on a new alternative fuel, DME (Dimethyl Ether), from the energy security and the environmental aspects. DME is a new synthetic fuel and the most simple ether compound, expressed by the chemical formula, $CH_3OCH_3$. Recently, the direct synthesis process of DME from CO and $H_2$ are being reformed from the coal gasfication(1). Thus, DME can be produced from any kinds of carbon resources, such as natural gas, coals and coal-bed methane associated in the coal mine.

DME does not contain sulfur component and is quite suitable for diesel engine because of high cetane number and no emission of suspended particle matters. Adiabatic flame temperature is sufficiently high, but DME has rather low ignition temperature with high burning velocity compared with propane and methane. This fact causes difficulty in the use of pre-mixed system for low-NOx combustion. In order to develop combustion technology of DME for boilers and gas turbines, it is essential to introduce new and alternative concept for low-NOx combustion(2).

Diffusion burner is required to be used in DME combustion, yet the diffusion burner has high potential of NOx emission. Thus it may be necessary for low NOx combustion to introduce even partly a premixed process very close to the burner plate for flame holding. At the same time, the large flame leading to an appearance of hot spot must be avoided by introducing segmented flame.

This study focuses on the fundamental characteristics of DME combustion, aiming at the development of low-NOx multi-port burner suitable for the tube-nested combustor. The tube-nested combustion(3) is a concept of the low-NOx combustion. In the conventional boiler, the water tubes are installed as a membrane water-wall surrounding a furnace. In the tube-nested combustor, the water tubes are moved into the furnace closely to the burner and cool down the burning flame directly in the field of burning reaction. Agitation of the burning flame with the installed water-tube-nest enhances combustion and brings about a uniform flame temperature distribution leading to the NOx reduction. To prevent the unburned combustibles emission by the flame quenching on the water tube surface, the burner used in the tube-nested combustor needs a high performance of mixing at the burner exit.

Multi-port burner consists of multiple small holes for gaseous fuel and air supply. A burner unit consists of a centered fuel-port and air-ports. On a small scale, the strong re-circulation flow is formed by the small jet unit, thus the fuel-air mixing is enhanced and the small flames form a cluster on every burner unit so that the thermal NOx and CO emissions are significantly suppressed to a very

* Received 30th September, 2005 (No. 05-4182)
** Department of Mechanical Engineering, Kansai University, 3–3–35 Yamate-cho, Suita, Osaka 564–8680, Japan. E-mail: matumoto@kansai-u.ac.jp

low level.

In the course of the present development, first we conducted laboratory combustion test with the co-axial diffusion burner[4] and then with the newly designed multi-port burner. Numerical simulation was also applied to investigate the mixing characteristics of fuel concentration. The clustered multi-port burner, which consists of three downsized multi-port burners, is examined to achieve the evenly distributed flame in the cross-section of the combustion chamber.

### Nomenclatures

$D_A$ : air hole diameter of multi-port burner
$D_G$ : fuel hole diameter of multi-port burner
$D_N$ : outer diameter of burner
$D_{out}$ : outer diameter of water tubes
$D_P$ : diameter of co-axial burner plate
$u_a$ : averaged air velocity air at the nozzle exit
$u_g$ : averaged fuel velocity at the nozzle exit
$\phi$ : equivalence ratio
$\rho_a$ : density of air
$\rho_g$ : density of fuel

## 2. Experimental Apparatus

### 2.1 Experimental setup

Figure 1 shows the experimental setup for the diffusion combustion. Main parts consist of a blower, orifice flow meters and a diffusion combustor. City gas is supplied from a gas piping equipped in the laboratory, while the DME and LPG (liquefied petroleum gas, 99% of propane and 1% of ethane) are supplied as a gas state from a gas cylinder. The purity of the DME gas is 99.9%. The city gas consists of 88% of methane, 6% of ethane, 3% of propane and 3% of butane and its low heating values is 41.6 MJ/m$^3_N$. The temperature of supplied fuel gas is room temperature.

The combustor, shown in Fig. 2, consists of the diffusion burner and the combustion chamber equipped with water tubes. The combustion chamber has a cross-section of 100 mm × 90 mm and 582 mm in height. At the bottom of chamber, the diffusion burner is installed. All the inner walls of the chamber are covered with fireproof materials. All the metallic parts of the setup consist of SUS304. In the combustion chamber, the water tubes with an outer diameter of $D_{out}$ = 13.8 mm are arranged in the 5×5 in-line array with the tube spacing of $H/D_{out}$ = 1.6 and $L/D_{out}$ = 2.0 in a transverse and a stream-wise directions, respectively. The heat transfer rate from the burning gases to the tube banks is calculated from the cooling water flow rate and the temperature difference between the outlet and the inlet. Thus obtained heat transfer rate was kept nearly constant at about 4 – 5 kW.

The combustion gases are sampled at 530 mm from the burner exit by using a water-cooled sampling probe. The combustion gas is analyzed by the gas analyzer (Horiba Corp. PG-235a). The CO, NOx, and $O_2$ concentrations are measured by infrared absorption, chemiluminescence, and zirconia oxygen sensor, respectively. The gas temperature is measured by R-type thermocouple at the same position.

The diffusion burners consists of outer cylinder with $D_N$ = 55 mm in I.D. and inner gas-supply cylinder with 21.7 mm O.D., and air flows through this annular gap. The heat release rate is kept constant at 11.6 kW except the experiments on the clustered multi-port burner.

### 2.2 Burner plate

Two types of burner plates were examined in the present experiments. The first one is referred to as 'co-axial burner', as shown in Fig. 3 (a). The combustion air is issued in the form of annular jet and the fuel gas from the center hole. To improve flame holding, eight air holes of 1.5 mm in diameter are arranged on the burner plate around the center fuel hole. The second burner plate

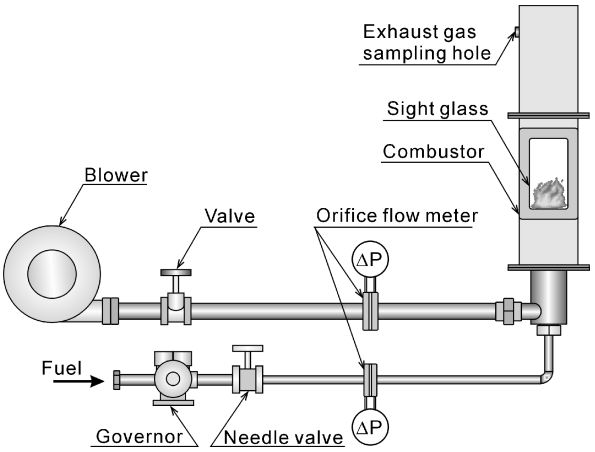


Fig. 1 Experimental setup

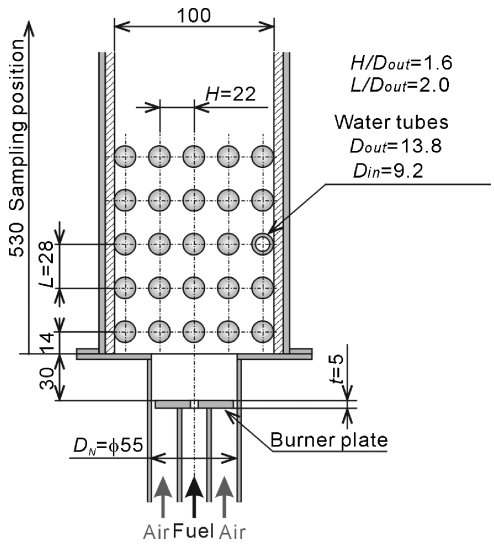


Fig. 2 Combustion chamber with water tube-nest, scale in mm

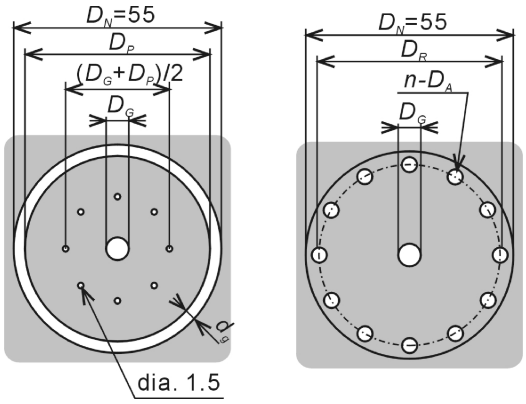


(a) Co-axial (b) Multi-port

Fig. 3 Burner plates of diffusion burner, scale in mm

Table 1 Dimensions of burner plate, scale in mm

| Co-axial burner | | Multi-port burner |
|---|---|---|
| $D_G$ / $D_P$ | Annular gap $d_g$ | $D_G$ / $n$-$D_A$ |
| 3 / 47 | 4 | 4 / 12-4 |
| 4 / 47 | 4 | 4 / 18-4 |
| 4 / 50 | 2.5 | 5 / 6-4 |
| 5 / 45 | 5 | 5 / 12-4 |
| 5 / 47 | 4 | 6 / 12-4 |
| 5 / 50 | 2.5 | 7 / 12-4 |
| 5 / 51 | 2 | 8 / 12-4 |
| 5 / 52 | 1.5 | 3 / 24-2 |
| 6 / 47 | 4 | 4 / 24-2 |
| 6 / 50 | 2.5 | 5 / 24-2 |
| 6 / 51 | 2 | 6 / 24-2 |
| 7 / 47 | 4 | 7 / 24-2 |
| | | 8 / 24-2 |

shown in Fig. 3 (b) is referred to as 'multi-port burner', which is an improved type from the former one, aiming at low-NOx combustion, i.e. this plate is so designed as to achieve well-mixed condition of fuel gas, steady and strong re-circulation followed by stable combustion and small but uniformly distributed flames. To increase air velocity, the total area of air-ports on the burner plate is reduced from that of co-axial burner. The annular gap of the former one is removed. Instead, small multiple ports are placed around the fuel port. The dimensions of these burner plates are listed in Table 1. The total of 12 co-axial burner plates and 13 multi-port burner plates were examined in this experiment. Every burner plates is installed 30 mm down the burner exit.

## 3. Results and Discussion

### 3.1 Co-axial diffusion burner

Figure 4 shows the NOx and CO concentrations of the flue gas of DME as a function of $O_2$ concentration from the co-axial diffusion burner with or without water

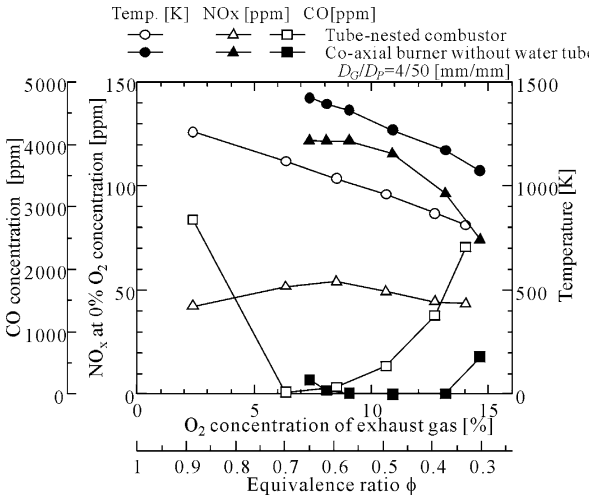


Fig. 4 Flue gas properties of DME combustor at 11.6 kW with co-axial diffusion burner of $D_G/D_P = 4/50$ [mm/mm]

tubes. In the previous report[4], the optimal burner plate has been selected among the burner listed in Table 1 based on the combustion tests without water tubes. The burner plate of $D_G/D_P = 4/50$ [mm/mm] shows a wide range of stable combustion for DME, LPG and the city gas. Measurements were carried out using the co-axial diffusion burner of $D_G/D_P = 4/50$ [mm/mm] at pre-determined heat release rate 11.2 kW by changing the air flow rate successively between the lift off limitation and the critical flame length (530 mm) determined from the length of the combustion chamber. The $O_2$ concentration of the flue gas is approximately related to the equivalence ratio by $\phi = (21 - O_2[\%])/21$.

Figure 4 shows the typical characteristics of the tube-nested combustion. The flue gas properties of the co-axial burner without water tubes have high NOx emission of around 120 ppm, however, the CO emission is low enough in the wide equivalence ratio. By applying the tube-nested combustor, NOx emission is reduced to about 50 ppm. The water tubes cool down the burning flame directly so that the local high-temperature point in the furnace vanishes and the uniform temperature distribution is achieved[4]. The temperature of the flue gas is decreased of about 320 K by applying the tube-nested combustor. The ranges of stable combustion become wider than that without water tubes at the high equivalence ratio. Matsumoto et al.[5],[6] reported that the flow pattern in the tube-nested combustor was dominated by the tube arrangement, especially near the burner exit. The tube banks causes a strong re-circulation at the burner exit and then enhances the mixing. However, the CO emission is higher than the acceptable range except at the equivalence ratio $\phi = 0.7$. At a low equivalence ratio $\phi < 0.7$, the burning gas is excessively cooled by the water tubes due to high heat transfer performance of burning gas. At the high equivalence ratio $\phi = 0.9$, the CO emission increases because of the weak

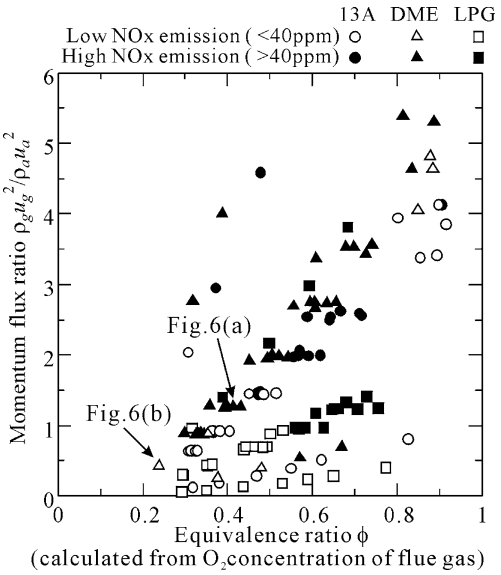


Fig. 5 Relationship between momentum flux ratio and NOx emission in the tube-nested combustor with co-axial burner

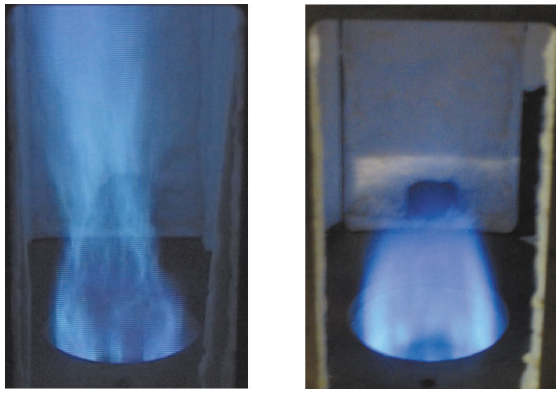

(a) Stable flame
$\phi = 0.40$, $\rho_g u_g^2/\rho_a u_a^2 = 1.4$
$u_g = 16.4$ m/s, $u_a = 17.8$ m/s

(b) Suppressed flame
$\phi = 0.22$, $\rho_g u_g^2/\rho_a u_a^2 = 0.43$
$u_g = 16.4$ m/s, $u_a = 32.1$ m/s

Fig. 6 Flame patterns of DME combustor with co-axial burner $D_G/D_P = 4/50$ [mm/mm]

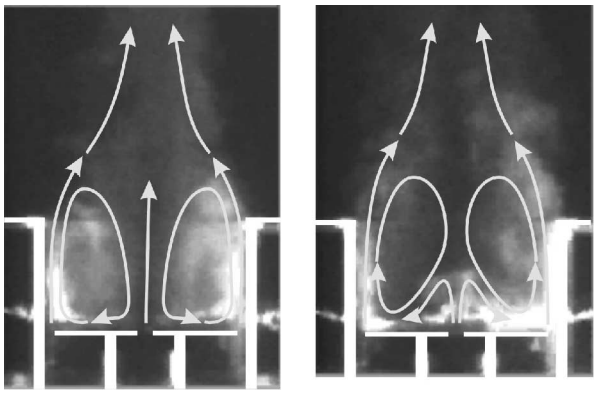

(a) $\rho_g u_g^2/\rho_a u_a^2 = 1.22$
$u_g = 27.5$ m/s, $u_a = 24.8$ m/s

(b) $\rho_g u_g^2/\rho_a u_a^2 = 0.48$
$u_g = 17.1$ m/s, $u_a = 24.8$ m/s

Fig. 7 Flow pattern in co-axial burner model $D_G/D_P = 4/50$ [mm/mm]

fuel-air mixing by the low air-velocity at the burner exit. The tube-nested combustor has a relatively narrow combustible range with low-NOx and low-CO emissions, as shown in Fig. 4.

For further NOx and CO reduction, it is necessary to improve the performance of the diffusion burner. Figure 5 shows the relationship between the momentum flux ratio and the equivalence ratio including the data of all the co-axial burner plates with the water tubes. The open plots indicate low-NOx emission less than 40 ppm. Momentum flux ratio, $\rho_g u_g^2/\rho_a u_a^2$, is the ratio of momentum fluxes of the fuel-gas jet to the annular air-jet. $u_g$ and $u_a$ are the area averaged velocities at the nozzle exit. $\rho_g$ and $\rho_a$ are the density of fuel and air, respectively. In this type of diffusion burner, the re-circulation occurred at the burner plate plays an important role for the flame holding and the fuel-air mixing[7]. The low-NOx emission is realized at low momentum-flux ratio less than one. At low momentum-flux ratio, however, the flame pattern becomes unstable[4]. Figure 6 shows the flame patterns of DME. At high momentum-flux ratio, $\rho_g u_g^2/\rho_a u_a^2 = 1.4$, Fig. 6 (a), stable combustion flame was observed. However, at high air ratio, i.e. at low momentum-flux ratio, Fig. 6 (b), the flame becomes short and partially lifts.

Flow visualization photographs are shown in Fig. 7. This flow visualization was carried out in the cold model facility with the smoke wire method. The working fluid was air. The momentum flux ratio, which is the key parameter for the flow pattern[4], corresponds to those of Fig. 6. At high momentum flux ratio, i.e. high velocity of the fuel-jet, the fuel-jet flows through the re-circulation, as shown in Fig. 7 (a), thus the fuel-air mixing is not suitable. However, the pilot flames formed at the eight small holes of 1.5 mm diameter causes the stable and long flame, as shown in Fig. 6 (a). At low momentum flux ratio, however, the fuel-jet is suppressed by the re-circulation, and then does not flow through the re-circulation. The fuel-jet is bent by the strong re-circulation at low momentum-flux ratio and becomes unstable as shown in Fig. 7 (b), then the flame holding is also unstable, but the fuel is mixed in the re-circulation and flame length becomes short, which is appropriate for low NOx emission and low CO emission. The improvement of burner plate must be investigated to solve such conflicts between the mixing problem, flame length and flame holding. The multi-port burner is one of the solutions for the mixing problem and flame holding problem for such conflicts.

### 3.2 Numerical simulation on multi-port burner

Numerical simulations with Phoenics Ver.3.4 are performed to investigate the velocity and concentration field at a non-reacting condition. The burner plate model is shown in Fig. 8, which has 7 central ports and 42 surrounding ports of 1.2 mm in diameter in hexagonal arrangement.

The working fluid is air, however, the Schmidt number is set at $Sc = 0.672$, which corresponds to the diffusion of methane in air. The computational domain has 70 mm in streamwise length. The boundaries of computational domain are free outlet conditions. The number of grids is about 1 600 000. The steady solutions for turbulent flow field are calculated with standard k-ε model.

Figure 9 shows the velocity field (b) and concentration field (c) at two different momentum flux ratios, $\rho_g u_g^2/\rho_a u_a^2 = 1.0$ and 0.11. Flow visualization experiments with the same geometric burner plate were carried out by smoke wire method as shown in Fig. 9 (a). The vector maps of the simulation results are consistent with the experimental results. In terms of the multi-port burner, the flow pattern is classified into two patterns: the penetration flow and the suppressed flow similar to the flow patterns in Fig. 7.

In Fig. 9 (b), at high momentum-flux ratio, the central jets flow through the re-circulations. The jets from the central and ambient ports merged together at $z = 10$ mm, and the velocity profile becomes almost uniform. The concentration field indicates the concentration of gas from the center jets. The mixing at high momentum-flux ratio is weak, because mixing occurred downstream of the re-circulations zone. This weak mixing causes a long flame pattern as shown in Fig. 6 (a). On the contrary, the suppressed flow pattern at low momentum-flux ratio has large and strong re-circulations. Mixing occurs in the re-circulation zone. The suppressed flow pattern has a high performance of mixing.

Figure 10 shows the flow pattern map obtained in the simulation model Fig. 8. At low momentum-flux ratio, the suppressed flow pattern is observed. From Fig. 10, the flow pattern is decided by the momentum-flux ratio and is independent of the air velocity $u_a$. The same results are obtained by the flow visualization of co-axial burner as shown in Fig. 7.

This simulation model has 2 rows of surrounding air-jets on the burner plate. However, the outer-row surrounding-jets have almost no contribution to the mixing with fluid from central-jets, as shown in Fig. 9 (c). In the experiments, therefore, the ambient ports are arranged in one row as shown in Fig. 3 (b).

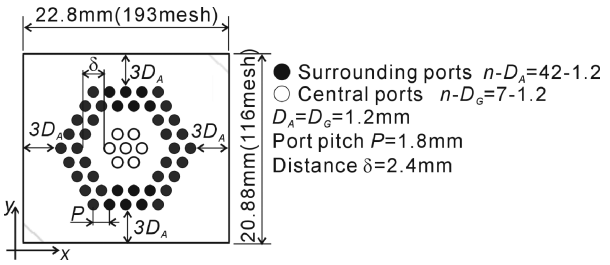


Fig. 8 Simulation model of multi-port burner

### 3.3 Combustion test with single multi-port burner

Figure 11 shows the NOx and CO concentrations of the flue gas of DME as a function of $O_2$ concentration. Data include all the multi-port burners without wa-

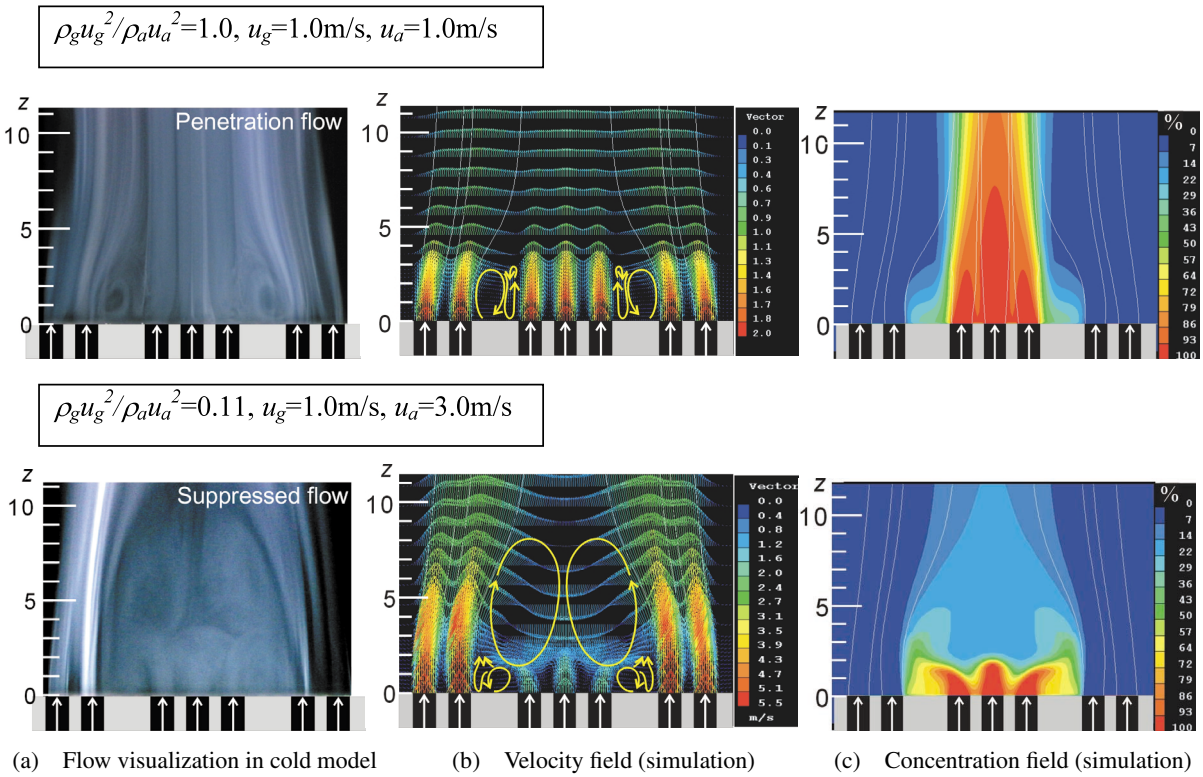


(a) Flow visualization in cold model (b) Velocity field (simulation) (c) Concentration field (simulation)

Fig. 9 Velocity and concentration field along the centerline of simulation model

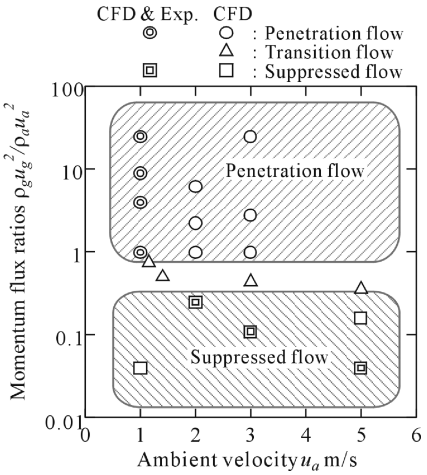


Fig. 10 Flow pattern map of multi-port burner model

ter tubes. The open circle plots with dashed line indicate the flue gas properties of co-axial burner with $D_G/D_P = 4/50$ [mm/mm]. The NOx emission of the multi-port burner is reduced to around 60 ppm at 0% $O_2$ concentration. The area of air-jets on the multi-port burner plate decreases to 18 – 73% of that of $D_G/D_P = 4/50$ co-axial burner, thus the high air velocity and low momentum-flux ratio induce a good mixing condition. The momentum flux ratios at these combustion conditions are sufficiently low at about 0.01 to 0.8. The CO concentration is also adequate. The distributions of CO emission show a unique relationship to $O_2$ concentration throughout all multi-port burners in Fig. 11.

The relationship of the NOx emission and air velocity is shown in Fig. 12, where the open plots indicate the low CO emission and the solid plots means the high CO emission over 500 ppm. Plots are classified into three groups by the burner type and air-ports diameter $D_A$. In the case of co-axial burner, NOx concentration decreases with the air velocity, however, high CO emission occurs at low NOx concentration less than 60 ppm, being considered as due to the transition of the flow pattern from the penetration flow to the suppressed flow. Applying the multi-port burner with the air-ports diameter of $D_A = 4$ mm, the NOx concentration slightly decreases with the air velocity, however, the NOx emission does not decrease with the air velocity of over 40 m/s. In the case of $D_A = 2$ mm, the NOx concentration is almost constant against the air velocity. The use of this type of multi-port burner, therefore, results in further increase in the air velocity, thus further reduction in the air-ports area on the burner plate has no significance for the NOx reduction.

In Fig. 11, the combustible range of the multi-port burner expands to low air ratio. The burner plates $D_G/n - D_A = 6/12 - 4$ and $5/24 - 2$ show the lowest NOx emission in the multi-port burner plates and the burner plate $D_G/n - D_A = 4/18 - 4$ has a good flame stability. Figure 13 shows the flame pattern of these burner plates. Multi-port

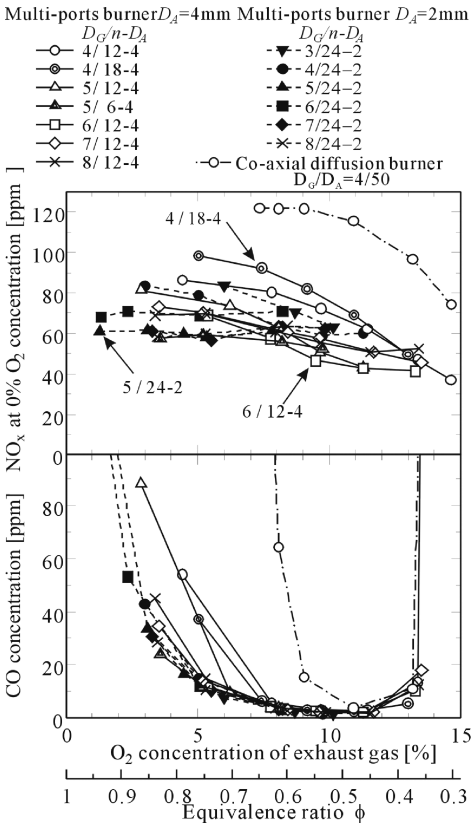


Fig. 11 Flue gas properties of DME combustion with multi-port burner, but without water tubes

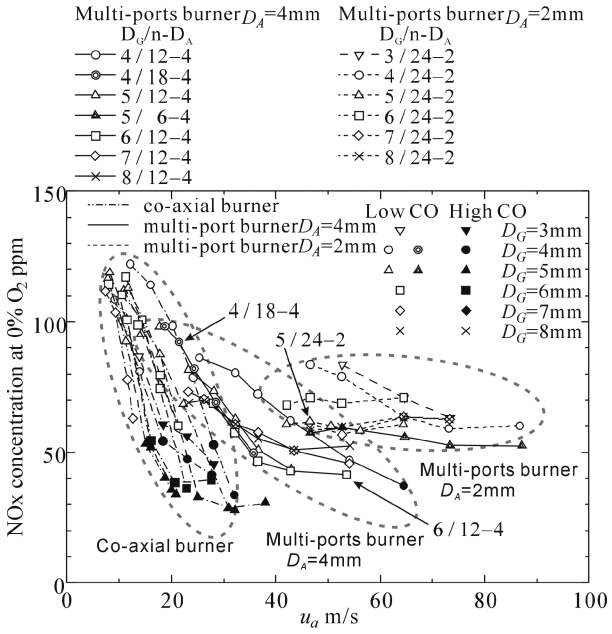


Fig. 12 Relationship between NOx emission and air velocity of DME combustion with multi-port burner, but without water tubes

burner has a high potential of flame holding even at high air velocity because of the small but uniformly distributed flames placed around the fuel port as shown in Fig. 13.

By applying the tube-nested combustion to three

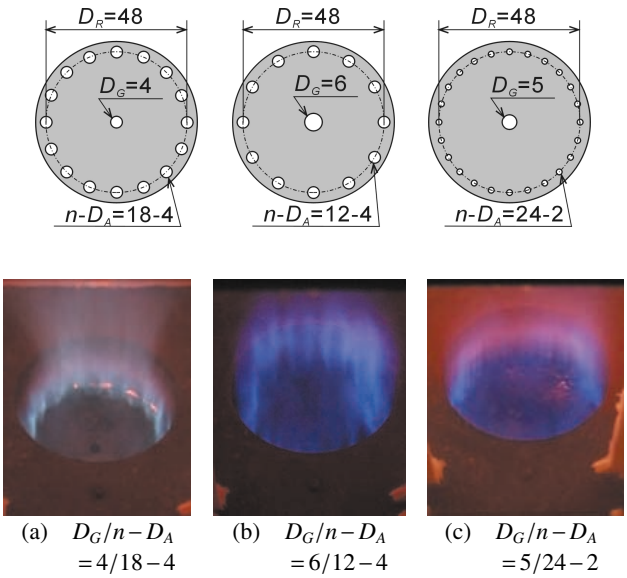


(a) $D_G/n-D_A = 4/18-4$ (b) $D_G/n-D_A = 6/12-4$ (c) $D_G/n-D_A = 5/24-2$

Fig. 13 Flame patterns of DME combustor with multi-port burner at $\phi = 0.67$

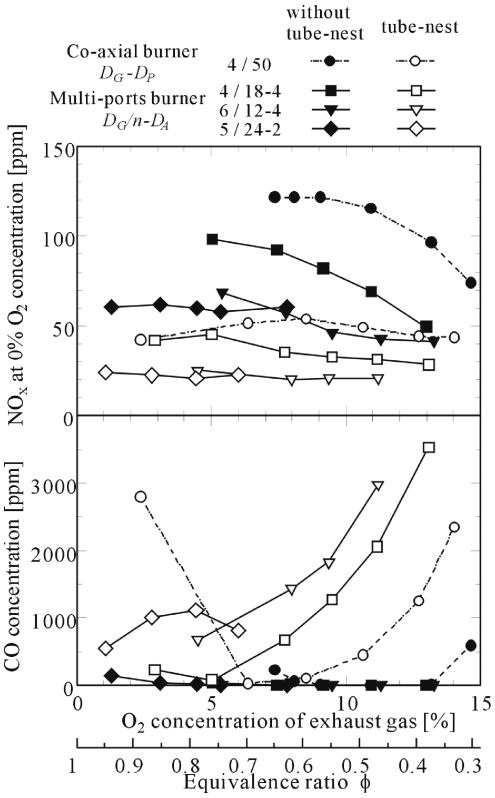


Fig. 14 Flue gas properties of DME combustor with multi-port burner installed in the tube-nested combustor

types of multi-port burner listed in Fig. 13. The NOx emission is reduced as shown in Fig. 14. The multi-port burner plate of $D_G/n-D_A = 4/18-4$ shows relatively low-CO (80 ppm) and low-NOx (45 ppm at $O_2$ 0%) emissions at the equivalence ratio $\phi = 0.76$. The equivalence ratio having the lowest CO emission shifted to the higher equivalence ratio, i.e. lower air-flow rate, than that of co-axial burner, because of the high mixing performance of

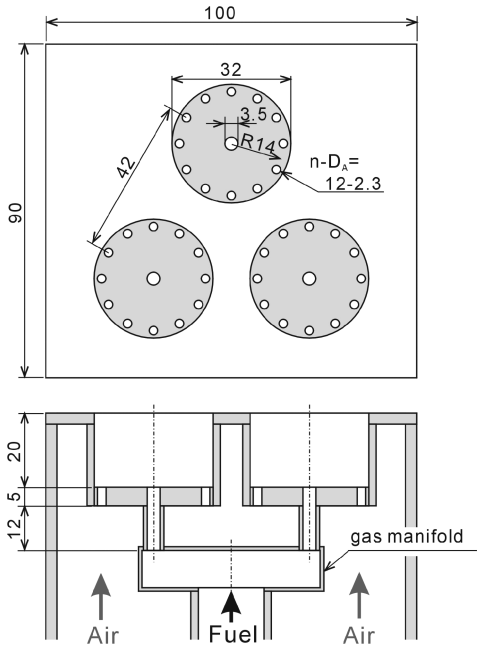


Fig. 15 Clustered multi-port burner

the multi-port burner. The burner plates of $D_G/n-D_A = 6/12-4$ and $5/24-2$ have about 20 ppm of NOx emission with the help of the tube-nested combustor, but the CO concentration is at a higher level than that of co-axial burner. In this experimental system, water flow rate in the tubes is kept high to avoid the boiling, then, CO emission become high due to the excess cooling by the water tubes. The CO concentration may be reduced by optimizing the water temperature of the water tubes.

### 3.4 Clustered multi-port burner

Clustered multi-port burner, which consists of three down-sized multi-port burners in this experiment, is designed to produce further uniformly distributed the small-flame and the burning gas velocity. The burning gas flowing uniformly into the water tube-banks prevents the local excessive cooling, thus the CO emission will be decreased. Segmentation of single burner into multiple burners brings about short mixing zone but with high performance of mixing and flame holding. Figure 15 shows the structure of the clustered multi-port burner with the three units of multi-port burner $D_G/n-D_A = 3.5/12-2.3$ in the equilateral triangle arrangement. One unit of this clustered multi-port burners has the flow area of one-third of the single multi-port burner $D_G/n-D_A = 6/12-4$, thus the total area of air and fuel ports are the same between them. The burner plates are installed 20 mm down the burner exit. The fuel gas is distributed through the gas manifold.

Figure 16 shows the flue gas properties of DME with clustered multi-port burner. The air velocity and the momentum flux ratio are the same with the single multi-port burner $D_G/n-D_A = 6/12-4$, therefore, the NOx and CO emissions of the clustered multi-port burner without the water tubes are almost the same that of the single multi-

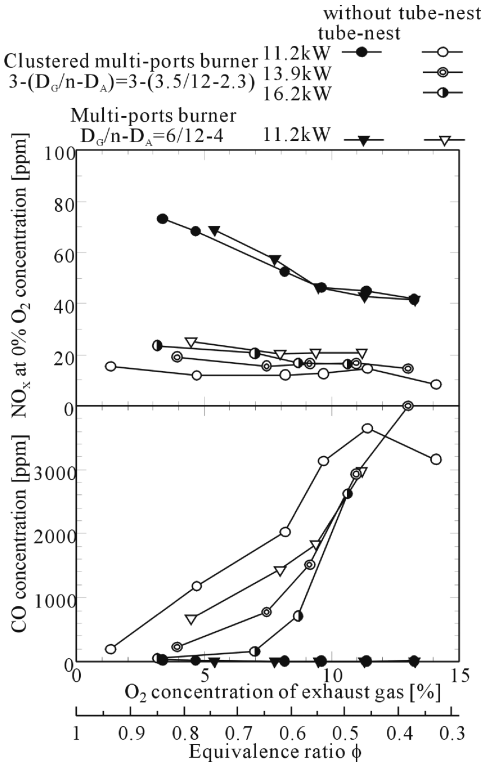


Fig. 16 Flue gas properties of DME combustor with clustered and single multi-port burner in the tube-nested combustor

port burner at the 11.2 kW heat release rate. By applying the tube-nest combustor, the NOx emission drastically reduced to about 18 ppm at 0% $O_2$ with 180 ppm of the CO emission at the equivalence ratio $\phi = 0.94$. However, the CO emission increases with decreasing the equivalence ratio. By increasing the heat release rate, the CO emission decreases. The heat transfer rate to the water tubes decreases relatively to the heat release rate, thus the excessive cooling is prevented. At the 16.2 kW, the low-NOx emission of about 25 ppm at 0% $O_2$ is achieved at the equivalence ratio from $\phi = 0.76$ to 0.85 with the CO emission less than 180 ppm. At the equivalence ratio $\phi = 0.85$, the NOx and CO emissions are 25 ppm at 0% $O_2$ and 51 ppm, respectively.

## 4. Conclusions

Experimental investigation on the DME combustion characteristics was conducted aiming at the development of low-NOx multi-port burner suitable for the tube-nested combustor. The results are summarized as follows:

( 1 ) Based on the co-axial diffusion burner, the NOx reduction from 130 ppm to 50 ppm at 0% $O_2$ is achieved with the help of the tube-nested combustor.

( 2 ) The numerical simulation indicates the high performance of mixing at low momentum flux ratio $\rho_g u_g^2/\rho_a u_a^2$.

( 3 ) Newly designed multi-port burner yields NOx emission of DME at about 60 ppm at 0% $O_2$. By applying the tube-nested combustion, NOx emission of DME is reduced to 45 ppm at 0% $O_2$.

( 4 ) Clustered multi-port burner with three units shows the low-NOx and low-CO emissions at 16.2 kW of the heat release rate. The low-NOx emission less than 25 ppm at 0% $O_2$ is achieved at the equivalence ratio from $\phi = 0.76$ to 0.85 with the CO emission less than 180 ppm.

## Acknowledgment

This study was conducted within the framework of the joint project of Kansai University and Hirakawa Guidam Co., Ltd. under the support by the Agency for Natural Resources and Energy, METI, Japan. The authors wish to express their sincere thanks to Messrs. S. Terada and I. Ikeda for their assistance in the experimental part of this DME project. Thanks are extended to JFE Holdings, Inc. for their support in carrying out this research. This research was partly supported by the Kansai University Grant-in-Aid for Promotion of Advanced Research in Graduate Course 2005.

## References

( 1 ) Ohno, Y., Ogawa, T., Shikada, T. and Inoue, N., DME Production Technology and Operation Results of 5 tons/day Plant, Proc. of the Int. DME Workshop, Japan DME Forum, (2000), pp.73–81.

( 2 ) Kobayashi, N., Inoue, H., Koizumi, H. and Watanabe, T., Robust Design of the Coaxial Jet Cluster Nozzle Burner for DME (Dimethyl Ether) Fuel, Proc. ASME TURBO EXPO 2003, GT2003-38410, (2993), CD-ROM.

( 3 ) Ishigai, S., Ozawa, M. and Ueda, Y., Application of 2nd-Generation JAFI Concept with Heat-Pipe-Tube Nest to Gas-Turbine Combustors for Gas-Firing, 21th Int. Congress on Combustion Engine CIMAC, Paper No.G10, (1995), pp.1–10.

( 4 ) Matsumoto, R., Ishihara, I., Ozawa, M. and Imahori, K., Development of Low-NOx Emission DME Combustor, JSME Int. J., Ser. B, Vol.47, No.2 (2004), pp.214–220.

( 5 ) Matsumoto, R., Shintani, Y., Okada, M., Imahori, K., Ohnishi, T., Ishihara, I. and Ozawa, M., Flow Pattern in a Simulated Tube-Nested Combustor, Trans. of the Visualization Society of Japan, (in Japanese), Vol.22, No.1 (2002), pp.15–22.

( 6 ) Matsumoto, R., Ohnishi, T., Ishihara, I. and Ozawa, M., Structure of Recirculation Flow Induced by an Annular Jet, Thermal Science and Engineering, Vol.11, No.2 (2003), pp.15–22.

( 7 ) Mizutani, Y. and Yano, K., Stability Condition and Attachment Mechanism of the Co-Axial Diffusion Flame, Trans. Jpn. Soc. Mech. Eng., (in Japanese), Vol.44, No.379 (1978), pp.1036–1052.